

AN APPROACH TO MULTI-RESOLUTION IN TIME DOMAIN BASED ON THE DISCRETE WAVELET TRANSFORM

C. Represa(*), C. Pereira(*), A.C.L. Cabeceira (**), I. Barba (**), J. Represa (**)

(*) Dpt. of Electromechanical Engineering. University of Burgos. 09001 Burgos. Spain.

Phone: +34 947258830 FAX: +34 947258831 E-Mail: crepresa@ubu.es

(**) Dpt. of Electricity and Electron. University of Valladolid. 47011 Valladolid. Spain.

Phone: +34 983423223 FAX: +34 983423225 E-Mail: ibarba@ee.uva.es

Abstract¹.- In this paper, an approach to multi-resolution in time domain (MRTD) is presented. Maxwell equations are discretized using finite differences in time and a derivative matrix in space that allows any desired level of spatial resolution. This derivative matrix acts on the coefficients that represent the expansion of the field components. These coefficients are calculated by means of the Discrete Wavelet Transforms (DWT). In this work hard (PEC and PMC) boundary conditions have been introduced into the algorithm using the method of images. This approach is valid for any kind of wavelet functions. Stability and dispersion properties are also investigated. Some numerical results, showing multi-resolution properties are presented.

Keywords.- Multi-resolution in time domain, MRTD, Daubechies wavelets, Discrete Wavelet Transform, DWT.

1.- Introduction

The development of electromagnetic fields in scale and wavelet functions [1], has given rise to the techniques known as Multi Resolution in Time Domain (MRTD). These techniques are based on the possibility of increasing the resolution of a signal, from a coarse level to a fine one, using low-resolution functions (scale functions), combined with others of intermediate resolution levels (wavelet functions). Different functions have been used in this type of analysis: Battle-Lemarie [2], Haar [3] or Daubechies [4].

In these techniques, the electric and magnetic field components of Maxwell's curl equations are represented by a manifold expansion in scale and wavelet functions with respect to space, and step functions with respect to time. The method of

moments [5] allows to obtain a set of equations similar to the one used in FDTD (identical, in the case of Haar functions, to the Yee's algorithm). Instead of the field values, the coefficients of this expansion are used in such scheme.

One of the points that affect the complexity of these schemes is the type of functions used for the expansion. For example, if Battle-Lemarié functions are used, an infinite number of coefficients must be used, because of the non-compact support of these functions. Actually, we can truncate the expansion and use a reduced number of them, obtaining an approximate solution. This problem does not appear when, for example, Haar functions are used, since they are compactly supported, so it is not necessary to truncate the expansion.

A second point is the desired resolution level for the solution of the problem. The above mentioned approaches [2-4] use scale functions for a first approximation of the fields; in this case simple functions are obtained, but, if an increasing of the resolution is desired, adding different levels of wavelet functions, the solution becomes unfeasible, as the scheme must be modified for every new level we add. This problem can be solved if a Discrete Wavelet Transform (DWT) is used to derive the coefficients of the expansions, as it has already been used to obtain the time domain solution of electrical networks [6]

In this work, compactly supported Daubechies wavelet functions [1] have been used to make an expansion of the fields. Its coefficients are computed through a Discrete Wavelet Transform. A derivative matrix, also obtained by means of a DWT, allows us to compute the value of the electric and magnetic fields at desired spatial positions and with the desired resolution. We have found the stability criterion of the algorithm for different wavelet functions and in some cases it is wider than the FDTD stability criterion for the

¹ This work was sponsored in part by the Spanish Ministry of Science and Technology, under its project TIC-2000-1612-C03-02.

same spatial resolution (twice in the case of Haar wavelet functions).

2.- Formulation

The simplest case of a TEM plane wave propagating in a homogeneous, linear, isotropic and non-dispersive media, with fields \mathbf{E}_x and \mathbf{H}_y is analyzed. Then, the equations to solve are:

$$\begin{aligned} \frac{\partial E_x}{\partial z} &= -\mu \frac{\partial H_y}{\partial t} \\ \frac{\partial H_y}{\partial z} &= -\varepsilon \frac{\partial E_x}{\partial t} \end{aligned} \quad (1)$$

In the proposed scheme, every field component is expanded in terms of scaling and wavelet functions, as shown in equation (2), where the coefficients of the lower resolution level (a_k^0) are given by the scaling function (ϕ) and the coefficients of the successive resolution level (b_k^j) are given by the wavelet functions (ψ):

$$F^n(z) = \sum_k^n a_k^j \phi_k^j(z) = \begin{cases} \sum_k^n a_k^0 \phi_k^0(z) \\ + \sum_{j=1}^{J-1} \sum_k^n b_k^j \psi_k^j(z) \end{cases} \quad (2)$$

The spatial discretization is achieved by dividing the domain into N cells of size Δ , as a starting point, then getting N sampling points in the center of each cell. This is what we call *resolution level 0* ($j = 0$). If each cell is now divided into 2^j points, the maximum level of desired resolution J ($j = J$) is reached and then the simulation domain has $N \cdot 2^J$

sampling points with a distance of Δz between them. This is illustrated in figure 1.

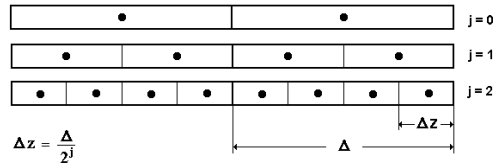


Fig. 1.- Spatial discretization for $J=2$.

The coefficients a_k^j are enough to represent the real values of the field at each sampling point and they are the initial and the final step of the decomposition process involved in the Discrete Wavelet Transform. The multi-resolution analysis performed with the wavelet transform can be understood as a digital filtering process where a signal is decomposed in two parts, one containing the low frequencies, the scale functions (ϕ), and other part containing the high frequencies, the wavelet functions (ψ). The multi-resolution representation through the Discrete Wavelet Transform (DWT) is provided by successive filter banks stages, each one containing a low-pass and a high-pass filter, described in terms of the coefficients of their impulse responses $L(m)$ and $H(m)$ ($m \in \mathbb{Z}$) respectively [1]. The filtering process means successive convolutions of the field and the filter coefficients followed by a decimation process that retains only the even indexes. The inverse transform (IDWT) consists in successive interpolations followed by convolutions that gives the field values using the coefficients of the previous decomposition. This is sketched in figure 2.

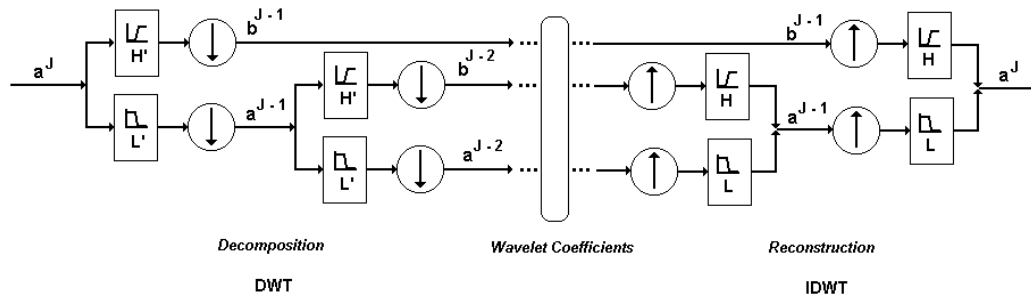


Fig. 2.- A step of the filtering process: the low and high-pass filters outputs the coefficients d and b^j respectively.

Then, eqs. (1) are discretized using centered finite differences for the time derivatives and a spatial derivative operator computed through a DWT matrix for the spatial derivatives. Each coefficient is, then, obtained from its values at the same point in a previous time step and from the derivation of

the other field coefficients at an intermediate time step:

$$\begin{aligned} H^{n+\frac{1}{2}} &= H^{n-\frac{1}{2}} - \frac{\Delta t}{\mu} \frac{1}{\Delta} \mathbf{D}^J (\mathbf{E})^n \\ \mathbf{E}^{n+1} &= \mathbf{E}^n - \frac{\Delta t}{\varepsilon} \frac{1}{\Delta} \mathbf{D}^J (\mathbf{H})^{n+\frac{1}{2}} \end{aligned} \quad (3)$$

where Δt and Δ are the time and space steps respectively, and \mathbf{D}^J represents the spatial derivative operator of level J . This operator [7] acts on the coefficients a and b of the field transform (3) and it is denoted by a matrix \mathbf{D} [8] which can be computed previously. In this way, eqs. (3) can be rewritten as follows for an arbitrary level of resolution J :

$$\begin{aligned} \begin{bmatrix} \mathbf{E}^{\psi^j} \\ \mathbf{E}^{\phi^0} \end{bmatrix}^{n+1} &= \begin{bmatrix} \mathbf{E}^{\psi^j} \\ \mathbf{E}^{\phi^0} \end{bmatrix}^n - \frac{\Delta t}{\varepsilon} \frac{1}{\Delta} \mathbf{D}^J \begin{bmatrix} \mathbf{H}^{\psi^j} \\ \mathbf{H}^{\phi^0} \end{bmatrix}^{n+\frac{1}{2}} \\ \begin{bmatrix} \mathbf{H}^{\psi^j} \\ \mathbf{H}^{\phi^0} \end{bmatrix}^{n+\frac{1}{2}} &= \begin{bmatrix} \mathbf{H}^{\psi^j} \\ \mathbf{H}^{\phi^0} \end{bmatrix}^{n-\frac{1}{2}} - \frac{\Delta t}{\mu} \frac{1}{\Delta} \mathbf{D}^J \begin{bmatrix} \mathbf{E}^{\psi^j} \\ \mathbf{E}^{\phi^0} \end{bmatrix}^n \end{aligned} \quad (4)$$

where $j=0, \dots, J-1$. This matrix \mathbf{D} is banded with a limited band width, due to the compact support of the Daubechies wavelets, and this width increases as the size of the filters does. Its elements are integrals of the scaling and wavelet functions and its discrete spatial translations of the first derivative (eqs. (6.1)-(6.4)). Because of multi-resolution, this matrix can be decomposed in a set of submatrices of lower resolution, so if we have named the original matrix of highest resolution \mathbf{D}^J , it is constructed with the one level lower matrices \mathbf{A} , \mathbf{B} , $\mathbf{\Gamma}$, \mathbf{D} , then:

$$\mathbf{D}^J = \begin{pmatrix} \mathbf{A}^{J-1} & \mathbf{B}^{J-1} \\ \mathbf{\Gamma}^{J-1} & \mathbf{D}^{J-1} \end{pmatrix} \quad (5)$$

where $\mathbf{A}^j = \{\alpha_{ij}^j\}$, $\mathbf{B}^j = \{\beta_{ij}^j\}$, $\mathbf{\Gamma}^j = \{\gamma_{ij}^j\}$, $\mathbf{D}^j = \{d_{ij}^j\}$. The components of every matrix can be calculated in a recursive way, so:

$$\alpha_{ij}^j = 2^j \alpha_{i-1}^j \quad (6)$$

and similar expressions for the other coefficients, β , γ and d . The expression α_1 is obtained by means of the following expression:

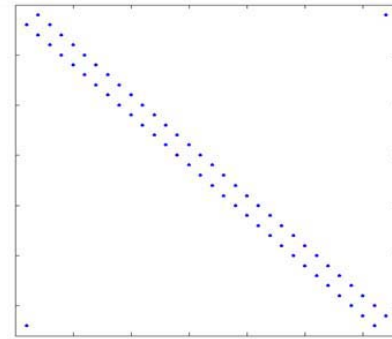
$$\alpha_1 = \int \psi(z-1) \cdot \frac{d}{dz} \psi(z) \cdot dz \quad (7)$$

Similar expressions, combining scale and wavelet functions can be used to calculate the other coefficients β (scale, wavelet), γ (wavelet and scale) and d (scale and scale). The scale and wavelet functions in every case are obtained by means of the low-pass and the high pass filters, $L(m)$ and $H(m)$ respectively:

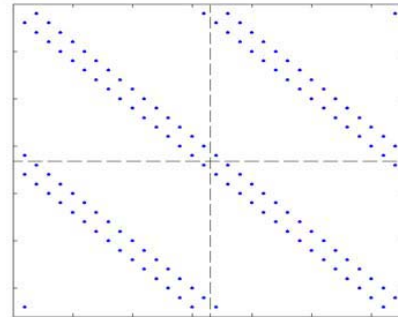
$$\phi(t) = \sum_{m=0}^{L_f-1} L(m) \sqrt{2} \phi(2t-m) \quad (8)$$

$$\psi(t) = \sum_{m=0}^{L_f-1} H(m) \sqrt{2} \phi(2t-m) \quad (9)$$

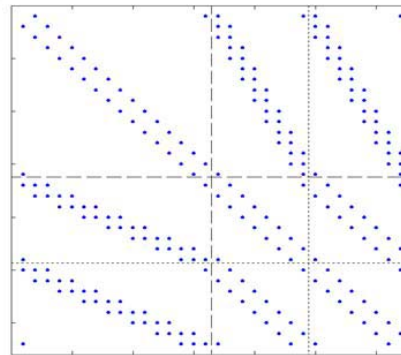
being L_f the filter length. In figure 3 three different aspects of the derivative matrix \mathbf{D} for three levels of resolution are depicted, where only the nonzero elements have been plotted.



(a)



(b)



(c)

Fig. 3.- Three different aspects of the derivative matrix \mathbf{D}^j for three resolution levels: (a) $j=0$, (b) $j=1$, (c) $j=2$.

The use of this derivative matrix allows us to achieve any level of resolution without modifications of the algorithm. Moreover, we can choose at the beginning of the simulation what type

of wavelet function is going to be used, and what regions of the simulation domain we want to solve at higher resolution. This feature will be shown further in the examples.

3.- Boundary conditions.

The derivative matrix \mathbf{D} is built-up in a cyclic form in such a way that it treats the coefficients on both boundaries as contiguous. It results in a cyclic space, that is, an infinite unbounded space. As the simulation domain is not cyclic at all, the character of the matrix must be modified. To do so, we propose to add adjacent columns with the elements related to the boundaries, and getting an *extended matrix*; i.e.

$$\{\alpha_{ij}\} = \begin{pmatrix} \alpha_0 & \alpha_{-1} & 0 & \alpha_1 \\ \alpha_1 & \alpha_0 & \alpha_{-1} & 0 \\ 0 & \alpha_1 & \alpha_0 & \alpha_{-1} \\ \alpha_{-1} & 0 & \alpha_1 & \alpha_0 \end{pmatrix}$$

↓

$$\{\alpha_{ij}\}_{\text{extended}} = \left(\begin{array}{cccc|cccc} \alpha_1 & \alpha_0 & \alpha_{-1} & 0 & 0 & 0 & 0 & 0 \\ 0 & \alpha_1 & \alpha_0 & \alpha_{-1} & 0 & 0 & 0 & 0 \\ 0 & 0 & \alpha_1 & \alpha_0 & \alpha_{-1} & 0 & 0 & 0 \\ 0 & 0 & 0 & \alpha_1 & \alpha_0 & \alpha_{-1} & 0 & 0 \end{array} \right)$$

and similar expressions for $\{\beta\}$, $\{\gamma\}$, and $\{d\}$. The matrix \mathbf{D} acting on the column vector $(\mathbf{b}^J, \mathbf{a}^J)$ at resolution level J implies that its extension must act on an extended vector too. The additional coefficients needed to represent the boundaries can be obtained using the method of images for PEC or PMC walls. If d'_L and b'_L are the scale and wavelet coefficients respectively, belonging to a border cell collocated at position $\mathbf{z}=L\Delta\mathbf{z}$, we obtain the additional coefficients a' and b' this way:

- for even symmetry:

$$\begin{cases} \mathbf{a}_{N+i}' = +\mathbf{a}_{N-i+1} \\ \mathbf{b}_{N+i}' = -\mathbf{b}_{N-i+1} \end{cases} \text{ on the right}$$

$$\begin{cases} \mathbf{a}_{1-i}' = +\mathbf{a}_i \\ \mathbf{b}_{1-i}' = -\mathbf{b}_i \end{cases} \text{ on the left}$$

- for odd symmetry:

$$\begin{cases} \mathbf{a}_{N+i}' = -\mathbf{a}_{N-i+1} \\ \mathbf{b}_{N+i}' = +\mathbf{b}_{N-i+1} \end{cases} \text{ on the right}$$

$$\begin{cases} \mathbf{a}_{1-i}' = -\mathbf{a}_i \\ \mathbf{b}_{1-i}' = +\mathbf{b}_i \end{cases} \text{ on the left}$$

These boundary conditions allow us to implement in a easy way infinite electric or magnetic walls.

More complex structures require more sophisticated techniques not studied here.

4.- Stability analysis

For the algorithm to be stable, the pair Δt and Δz must be chosen in a correct way. We choose these values following the derivation given in [9] where the stability problem is treated as an eigenvalue problem. This means that plane wave eigenmodes will be assumed to propagate in the numerical data space. The spectrum of eigenvalues for these modes due to the numerical space differentiation process will be determined and compared to the stable spectrum of eigenvalues determined by the numerical time differentiation process. By requiring the complete spectrum of spatial eigenvalues to be contained within the stable range, it is ensured that all possible numerical wave modes in the grid are stable. In this way, equations (1) can then be rewritten as follow:

$$\frac{H^{n+\frac{1}{2}} - H^{n-\frac{1}{2}}}{\Delta t} = -\frac{1}{\mu \cdot \Delta z} \sum_{\Gamma} d_i E_{i-1}^n \quad (10)$$

$$\frac{E^{n+1} - E^n}{\Delta t} = -\frac{1}{\varepsilon \cdot \Delta z} \sum_{\Gamma} d_i H_{i-1}^{n+\frac{1}{2}}$$

and this equations can be split into two eigenvalue problems concerning time and space:

$$\frac{H^{n+\frac{1}{2}} - H^{n-\frac{1}{2}}}{\Delta t} = \Lambda H_i^n \quad (11)$$

$$\frac{E^{n+1} - E^n}{\Delta t} = \Lambda E_i^{n+\frac{1}{2}}$$

$$-\frac{1}{\mu \cdot \Delta z} \sum_{\Gamma} d_i E_{i-1}^n = \Lambda H_i^n \quad (12)$$

$$-\frac{1}{\varepsilon \cdot \Delta z} \sum_{\Gamma} d_i H_{i-1}^{n+\frac{1}{2}} = \Lambda E_i^{n+\frac{1}{2}}$$

where only scaling functions of resolution level $J=0$ have been used. To avoid having any mode increasing without limit during normal time-stepping it is found from equation (11) that the stable spectrum of eigenvalues is:

$$|\text{Im}(\Lambda)| \leq 2 / \Delta t \quad (13)$$

In order to solve equations (12) we introduce a typical mode of the spatial spectrum like (14) into the equations:

$$\begin{aligned} {}^n E_i &= E_0 e^{j(\bar{k}_i \Delta z)} \\ {}^n H_i &= H_0 e^{j(\bar{k}_i \Delta z)} \end{aligned} \quad (14)$$

Then we get the following set of equations:

$$\begin{aligned} -\frac{1}{\mu \cdot \Delta z} \sum_I d_I E_0 e^{j(\tilde{k}+\Delta z)} e^{j(-\tilde{k}+\Delta z)} &= \Lambda H_0 e^{j(\tilde{k}+\Delta z)} \\ -\frac{1}{\varepsilon \cdot \Delta z} \sum_I d_I H_0 e^{j(\tilde{k}+\Delta z)} e^{j(-\tilde{k}+\Delta z)} &= \Lambda E_0 e^{j(\tilde{k}+\Delta z)} \end{aligned} \quad (15)$$

Simplifying and using Euler's identity we get that the spatial eigenvalues are given by:

$$\text{Im}(\Lambda) = \frac{c}{\Delta z} \sum_I d_I \text{sen}(-kl\Delta z) \quad (16)$$

Therefore, the maximum value of this eigenvalues is:

$$|\text{Im}(\Lambda)| \leq \frac{c}{\Delta z} \sum_I |d_I| \quad (17)$$

To guarantee numerical stability, the range of spatial modes must be contained completely within the stable range of time-stepping eigenvalues set by (17) and so:

$$\frac{c}{\Delta z} \sum_I |d_I| \leq \frac{2}{\Delta t} \quad (18)$$

Therefore, the upper bound of the time step Δt_{MRTD} is:

$$\Delta t_{\text{MRTD}} \leq \frac{2}{\sum_I |d_I|} \frac{\Delta z}{c} \quad (19)$$

Defining a stability factor like (20):

$$s = \frac{c\Delta t_{\text{MRTD}}}{\Delta z} \quad (20)$$

equation (19) establishes that the stability factor must be contained within the range :

$$0 < s \leq \frac{2}{\sum_I |d_I|} \quad (21)$$

Depending on the type of wavelet function used, this range implies that the time step can be set to a different value for the same spatial resolution. If Haar wavelet functions are used, this value can be set double than the time step set in FDTD for the same spatial resolution.

5.- Dispersion properties

The use of numerical techniques for solving electromagnetic problems as TLM [10], FDTD or MRTD require always a discretization process. Such a process result in a phase error of the field

propagation, that is, the numerical phase velocity given by the algorithm differ from the phase velocity of the wave in the medium [11]. This fictitious dispersive behaviour must be taken into account specially in considering large structures of simulation because significant differences between real and numerical phase can be obtained. Some studies about dispersion properties of MRTD methods based on Galerkin procedures [12], [13] have been done. Now we proceed to study the dispersion characteristics of the MRTD algorithm based on the DWT using Daubechies' wavelets functions. To do that, a plane monochromatic travelling-wave (22) is introduced into the discretized Maxwell equations (4) and then we search for the relationship between the angular frequency ω and the numerical wave number \tilde{k} :

$$\begin{aligned} {}^n E_i^\zeta &= E_0 e^{j(\tilde{k}\Delta z - \omega n \Delta t)} \\ {}^n H_i^\zeta &= H_0 e^{j(\tilde{k}\Delta z - \omega n \Delta t)} \end{aligned} \quad (22)$$

As starting point, we expand the field components using only scaling functions of resolution level $\mathbf{J}=0$, so $\zeta = \phi$ and the derivative matrix \mathbf{D}^0 will be composed of elements $\{d_{il}\}$. The discretized Maxwell equations can be written in this way:

$$\begin{aligned} {}^{n+1} E_i^\phi &= {}^n E_i^\phi - \frac{\Delta t}{\varepsilon} \frac{1}{\Delta z} \left[\sum_I d_I {}^{n+\frac{1}{2}} H_{i-1}^\phi \right] \\ {}^{n+\frac{1}{2}} H_i^\phi &= {}^{n-\frac{1}{2}} H_i^\phi - \frac{\Delta t}{\mu} \frac{1}{\Delta z} \left[\sum_I d_I {}^n E_{i-1}^\phi \right] \end{aligned} \quad (23)$$

Substituting (22) into (23), simplifying and using Euler's identity we get this set of equations:

$$\begin{aligned} 2E_0 \text{sen} \frac{\omega \Delta t}{2} &= \frac{\Delta t}{\varepsilon} \frac{1}{\Delta z} \left[\sum_I d_I H_0 \text{sen}(-\tilde{k}l\Delta z) \right] \\ 2H_0 \text{sen} \frac{\omega \Delta t}{2} &= \frac{\Delta t}{\mu} \frac{1}{\Delta z} \left[\sum_I d_I E_0 \text{sen}(-\tilde{k}l\Delta z) \right] \end{aligned} \quad (24)$$

and from them we obtain the dispersion relationship where c is the speed of light in our medium:

$$\frac{2\Delta z}{c\Delta t} \text{sen} \frac{\omega \Delta t}{2} = \sum_I d_I \text{sen}(-\tilde{k}l\Delta z) \quad (25)$$

This expression may be reduced to the ordinary expression $\omega = c\tilde{k}$, that is, the non-dispersive case, if spatial resolution Δz is very small in comparison with the wavelength. If Haar wavelet functions are used then we also obtain a non dispersive case at the stability factor $s = 2$ (i.e. the maximum stable value). In any case, dealing with broadband signals, different expressions will be obtained depending on the relation between the wavelength λ and the

spatial resolution Δz , and on the type of wavelet function we use. In figure 4 it is plotted the normalized phase velocity versus spatial resolution given by the expression (25) for two different values of the stability factor. We can appreciate the feature mentioned before, that is, the normalized phase velocity tend to unity as we increase the resolution. It can also be seen that the higher the order of the wavelet function, the better dispersion characteristics.

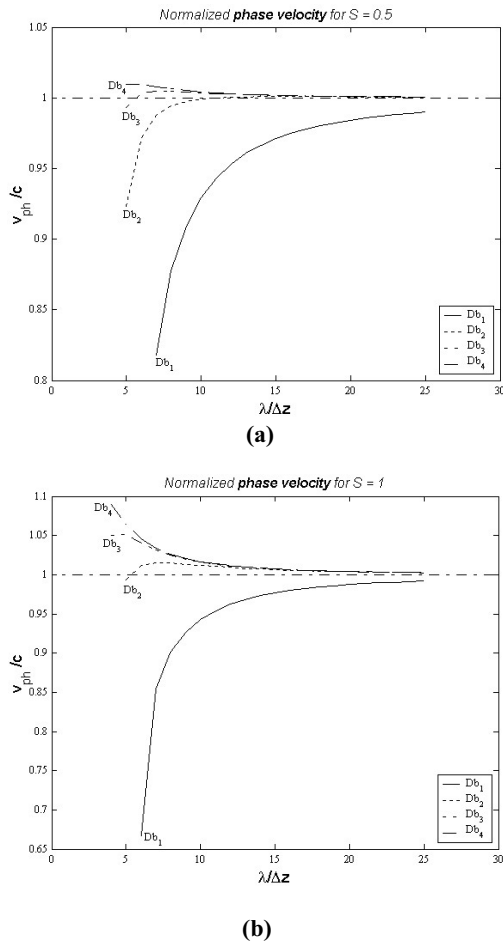


Fig. 4.- Normalized numerical phase velocity versus spatial resolution in lambda units for different wavelet functions:

- (a) with a stability factor $s=0.5$, and
- (b) with a stability factor $s=1.0$

In figure 5 it is depicted a gaussian pulse propagation using different types of wavelet functions: (a) Haar wavelet functions, and (b) Daubechies D_2 wavelet functions. The case (b) exhibit a better dispersive behaviour than the case (a) as it can be expected from previous figure 4.

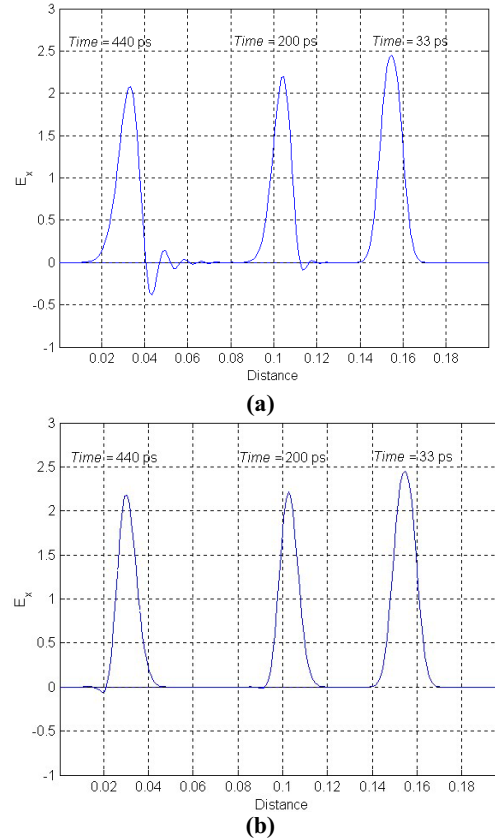


Fig. 5.- Three snapshots of a Gaussian pulse propagation using (a) Haar wavelet functions, and (b) Daubechies Db_2 functions, showing it dispersion properties.

6.- Results

To validate our proposed technique some additional examples have been performed. First of all we have evaluated the multi-resolution property of the algorithm. To do that, we have simulated a gaussian pulse excitation into a one-dimensional cavity of 1 m long. The simulation domain is split into two parts of different resolution, one of high resolution on the left side and 400 mm long, and other part of low resolution on the right side and 600 mm long. Figure 6 displays this simulation where it can be clearly seen the differences between the two parts. Figure 7 shows in detail the transition between zones.

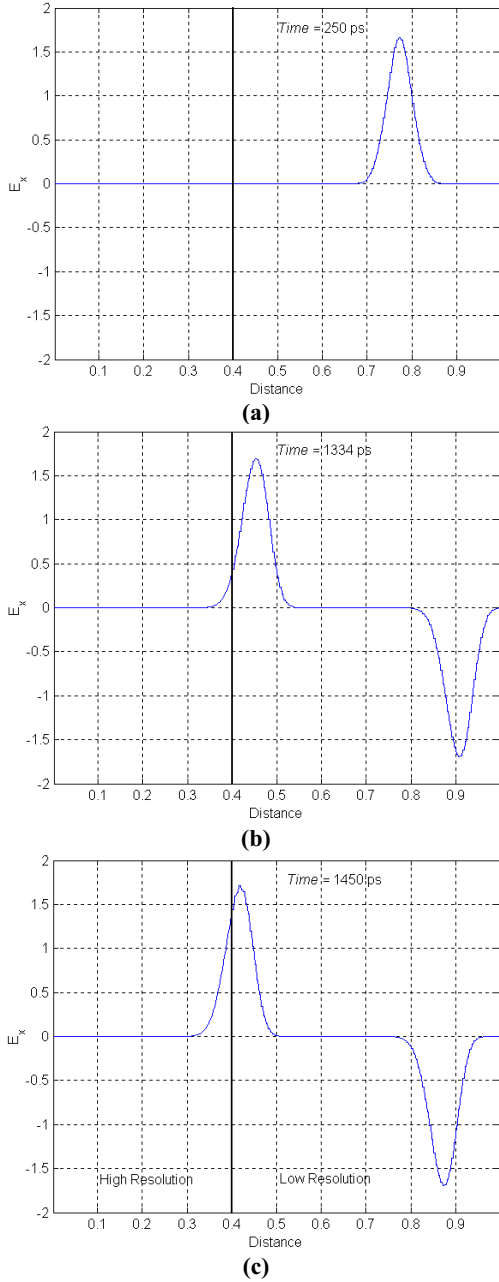


Fig. 6.- Gaussian pulse propagation using Haar wavelet functions. The simulation domain is split into two zones of different resolution.

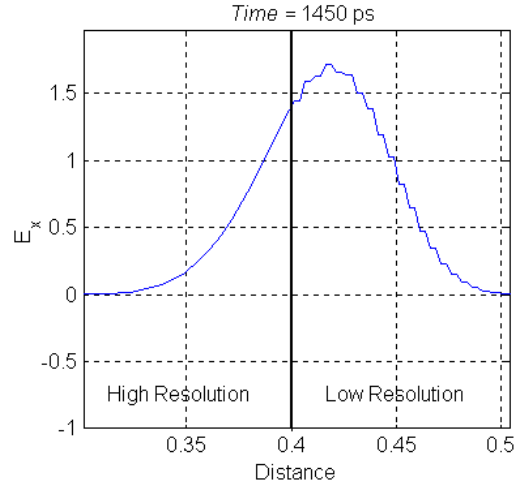


Fig. 7.- Details of the transition between two zones of different resolution.

We have also evaluated the resonant frequencies of a one-dimensional rectangular cavity with a 100 mm distance between electric walls (PEC). A spatial resolution of $\Delta z = 0.625$ mm and a time discretization of $\Delta t = 3.127$ ps have been chosen (that means, that, according to the stability criterion we choose $s = 1.5$). The electric and magnetic fields are specified at $t=0$ and at $t=1/2\Delta t$ respectively,

$$E_k^0 = \exp\left[-\left(\frac{k - k_c}{k_w}\right)^2\right] \quad (26)$$

$$H_k^{\frac{1}{2}} = \exp\left[-\left(\frac{k - k_c - s/2}{k_w}\right)^2\right] \quad (27)$$

where the width of the pulse is $k_w = 10$ and its center $k_c = 80$ in terms of the index of the spatial mesh. After 4096 time steps with a spectral resolution of $\Delta f = 78.1$ MHz, the resonance spectrum obtained have been plotted in figure 8

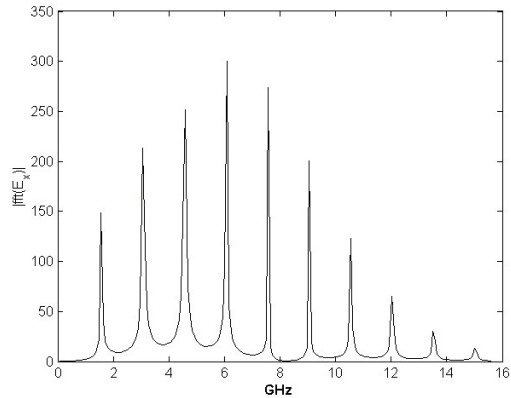


Fig. 8.- Resonant frequencies obtained in a cavity of length 100 mm using Haar wavelet functions.

7.- Conclusions

A new approach to Multi-Resolution in Time-Domain has been investigated. In this study a derivative matrix is used to calculate the spatial derivatives of the electromagnetic fields. This matrix acts on the coefficients of the wavelet expansions of the fields obtained from the Discrete Wavelet Transform. The use of this matrix allows us to solve the discretized Maxwell equations at any level of desired spatial resolution and wherever we may want. It has been shown that different types of Daubechies wavelet functions exhibit better dispersion properties for the same spatial resolution and that the time step can be chosen bigger than in other time-domain methods with the same mesh size. In this way, we can also choose at the beginning of the simulation different types of wavelet functions in order to improve our results.

9.- References

- [1] I. Daubechies, *Ten Lectures on Wavelets*, CBMS-NSF Ser. App. Math. 61, SIAM: Philadelphia 1992.
- [2] M. Krumpholz and L.P.B. Katehi, "MRTD: New Time-Domain schemes based on multiresolution analysis," *IEEE Trans. Microwave Theory Tech.* 1996; **44**(4):555-571.
- [3] M. Fujii and W.J.R. Hoefer, "A 3-D Haar-Wavelet-Based Multiresolution Analysis Similar to the FDTD Method – Derivation and Application –," *IEEE Trans. Microwave Theory Tech.* 1998; **46**(12):2463-2475.
- [4] Y. W. Cheong, Y. M. Lee, K. H. Ra, and C. C. Shin, "Wavelet-Galerkin scheme of time-dependent inhomogeneous electromagnetic problems," *IEEE Microwave Guided Wave Lett.* 1999, **9**(8):297-299.
- [5] R. F. Harrington, *Field Computation by Moment Methods*, IEEE Press: New York 1992.
- [6] S. Barmada and M. Raugi, "A general tool for circuit analysis based on wavelet transform," *Int. J. Circuit Theory and Applications.* 2000; **28**:461-480.
- [7] G. Beylkin, R. Coifman and V. Rokhlin, "Fast wavelet transform and numerical algorithms," *I. Comm. Pure Appl. Math.* 1991, **44**:141-183.
- [8] G. Beylkin, "On the representation of operators in bases of compactly supported wavelets," *SIAM J. Numer. Anal.* 1992; **6**(6):1716-1740.
- [9] A. Taflove, *Computational Electrodynamics: The Finite-Difference Time-Domain Method*, Artech House 1995.
- [10] C. Christopoulos, *The Transmission-Line Modelling Method: TLM*, IEEE MTT: New York 1995.
- [11] J. Represa, C. Pereira, M. Panizo, F. Tadeo, "A Simple Demonstration of Numerical Dispersion under FDTD," *IEEE Trans. Education.* 1997; **40**(1):98-102.
- [12] E.M. Tentzeris, R.L. Robertson, J.F. Harvey and L.P.B. Katehi, "Stability and Dispersion Analysis of Battle-Lemarie-Based MRTD Schemes," *IEEE Trans. Microwave Theory Tech.* 1999; **47**(7):1004-1013.
- [13] M. Fujii and W.J.R. Hoefer, "Dispersion of Time Domain Wavelet Galerkin Method Based on Daubechies' Compactly Supported Scaling Functions with Three and Four Vanishing Moments," *IEEE Microwave Guided Wave Lett.* 2000; **10**(4):125-127.



César Represa was born in Medina del Campo, Spain, in 1971. He received the *Licenciado* degree in Physics from the University of Valladolid in 1995, and the PhD degree in 2001 from the University of Burgos. He was *Profesor Asociado* at the University of Burgos from 1997 to 2000. Since 2000 he has been Assistant Professor at the University of Burgos. His research interest includes numerical methods in electromagnetics.



Carmen Pereira was born in Zamora, Spain, in 1951. She received the *Licenciado* degree in Physics in 1974, and the PhD degree in 1983, both from the University of Valladolid, Spain. She was Assistant Professor at the University of Valladolid from 1974 to 1985, and since 1985 has been *Profesor Titular* in Electromagnetics at the Universities of Valladolid and Burgos. Her current research interest includes numerical methods in electromagnetics and microwave devices.



Ana Cristina L. Cabeceira was born in Pontevedra, Spain, in 1969. She received the *Licenciada* Degree on Physics in 1992, and the Ph. D. Degree in 1996, both from the University of Valladolid, Spain. From 1992 to 1999 she was Assistant Professor,

then she become *Profesora Titular* in Electromagnetism of the University of Valladolid. Her main research interests include numerical methods for Electromagnetism, as well as characterization of electromagnetics properties of materials.



Ismael Barba was born in Palencia, Spain, in 1970. He received his *Licenciado* degree in Physics from the University of Valladolid in 1993. He received his MA degree in Electronical Engineering in 1995, and his PhD in Physics in 1997, all from the same University. He

was Assistant Professor from 1994 to 1999, and since 1999, he is *Profesor Titular* in Electromagnetics in the University of Valladolid. His main research interest includes numerical methods in electromagnetics, and characterization of electromagnetics properties of materials.



José Represa was born in Valladolid, Spain, in 1953. He received the *Licenciado* degree in Physics in 1976, and the PhD degree in 1984, both from the University of Valladolid, Spain. He was Assistant Professor from 1976 to 1985,

and since 1985 Professor in Electromagnetics at the University of Valladolid. His current research interest includes numerical methods in electromagnetics, characterization of electromagnetics properties of materials and microwave devices.

